




Dissipation-induced Liouville-Majorana modes in open quantum system

Xing-Shuo Xu , Xiang-Fa Zhou *, Guang-Can Guo, and Zheng-Wei Zhou [†]

CAS Key Lab of Quantum Information, University of Science and Technology of China, Hefei 230026, China;

Synergetic Innovation Center of Quantum Information and Quantum Physics,

University of Science and Technology of China, Hefei 230026, China;

and Hefei National Laboratory, University of Science and Technology of China, Hefei 230088, China



(Received 1 June 2022; revised 15 March 2023; accepted 5 September 2023; published 3 October 2023)

In open quantum systems, topological edge states rapidly lose coherence, making them unsuitable for topological quantum computation and quantum memory. In this study, we demonstrate that topologically non-Hermitian Liouville-Majorana edge modes (LMEMs) can persist in the extended Liouville-Fock space (LFS) of dissipative quantum spin or fermionic systems. This finding extends the scope of topological modes beyond typical Hermitian systems. By vectorizing the Lindblad equation of a dissipative Ising-type spin system using third quantization, we prove that it can be reduced to a series of non-Hermitian Kitaev chains in the extended LFS and that topologically protected LMEMs emerge due to internal symmetry. Furthermore, we present an explicit method for detecting these modes and demonstrate that the purity of the density matrix characterizes the long-range correlation of LMEMs. Our work offers a new direction for identifying stable topological states in open quantum systems induced by quantum jumps.

DOI: [10.1103/PhysRevResearch.5.043004](https://doi.org/10.1103/PhysRevResearch.5.043004)

I. INTRODUCTION

The realization and manipulation of topological quantum states has been a subject of enduring interest in various branches of physics [1–10]. Due to their nonlocal orders that are robust against local perturbations, topological phases offer intrinsic stability and may serve as ideal platforms for topological quantum computation and quantum memory. Moreover, these systems enable the construction of various quantum devices that cannot be covered by traditional materials [11–13].

However, topological phases are inevitably coupled to their surroundings in natural systems, resulting in quantum dissipation that can destroy these phases and contaminate the signals induced by their topological features [14–24]. Therefore, it is essential to search for novel, robust topological effects, even in dissipation, to implement various topological phases of matter and quantum computing tasks within current systems [25–28].

Recently, there has been a growing interest in talking about topological physics in non-Hermitian dissipative systems [29–38]. However, in most discussions, dissipation is characterized only by introducing an effective non-Hermitian Hamiltonian. The influence and back action of detections and quantum jumps on the dynamics of the system are only less

considered. For dissipative systems under the Markovian approximation, the general dynamics are governed by Lindblad equations [37–46], where both the dissipators and the influence of quantum jumps are explicitly considered. Although topological Majorana modes can be stationary states of the system by carefully designing the dissipative Lindblad operators, in general cases, Majorana modes are unstable in the presence of dissipation [26,47,48]. Therefore, it is natural to ask: What topological properties will be stable in dissipative systems?

Answering this question is a highly nontrivial task, as the master equation for dissipative many-body systems is still analytically and numerically challenging to solve [49–51]. Therefore, finding exactly solvable dissipative models with stable topological characteristics becomes a key ingredient in understanding nontrivial topological effects induced by dissipations, which is also less considered in current studies [52,53].

In this work, we present an analytically solvable dissipative Ising-type model (in spin language) or Kitaev chain described by Lindblad equation with site-dependent couplings and dissipations. Specifically, we vectorize the density matrix and map the Lindblad equation into a Schrödinger-like equation in the extended Liouville-Fock space (LFS) with an effective non-Hermitian Hamiltonian [42–44,48]. As a result, topological properties that are discussed for non-Hermitian Hamiltonians can also be applied to open quantum systems described by Lindblad equations. We note that although similar models have also been discussed in the literatures [52,53] using different methods on a periodic system, however, the topological properties of edge states and their detections in open system are less considered there, which will be the main focus of this work.

*xfzhou@ustc.edu.cn

[†]zwzhou@ustc.edu.cn

The main results of our study can be summarized as follows:

(1) We prove that for open boundaries, the system supports novel topological Liouville-Majorana edge modes (LMEM) in LFS, which is beyond the scope of the usual Hermitian Majorana modes discussed in a closed system.

(2) The proposed LMEMs are robust to symmetry-preserving disturbances and can be verified by examining fixed ratios of the mean values of carefully designed physical observables (product operators in LFS) over time evolution. Additionally, the correlations within LMEMs can be extracted through quadratic forms of physical observables [54–59].

(3) Our work highlights the significance of quantum jumps in creating new topological states in dissipative systems.

II. THE MODEL AND NON-HERMITIAN LIOUVILLIAN

We begin by examining the Lindblad equation governing the spin system under local dissipations ($\hbar = 1$)

$$i\dot{\rho} = [H, \rho] + i \sum_{j=1}^N \left(L_j \rho L_j^\dagger - \frac{1}{2} \{L_j^\dagger L_j, \rho\} \right), \quad (1)$$

where the Hamiltonian and Lindblad operators read

$$H = \sum_{j=1}^{N-1} J_j \sigma_j^x \sigma_{j+1}^x, \quad L_j = \sqrt{\gamma_j} \sigma_j^z. \quad (2)$$

Here J_j is the coupling strength between nearest-neighbor spins, and γ_j is the local dephasing rates. We stress that in the current system, all nontrivial dissipative dynamics can be attributed to the presence of quantum jump terms $L_j \rho L_j^\dagger$, since the relevant non-Hermitian Hamiltonian contains only homogeneous dissipations due to $L_j^\dagger L_j = L_j L_j^\dagger = \gamma_j I_j$.

In the absence of dissipation, the model can be solved by applying the celebrated Jordan-Wigner transformation, which is defined as

$$\sigma_j^x = \prod_{k<j} (-i w_{2k-1} w_{2k}) w_{2j-1}, \quad (3)$$

$$\sigma_j^y = \prod_{k<j} (-i w_{2k-1} w_{2k}) w_{2j}, \quad (4)$$

where w_j denotes the usual single-site Majorana fermion and satisfies $\{w_i, w_j\} = 2\delta_{ij}$. The Hamiltonian can then be written as

$$H = \sum_j J_j i w_{2j} w_{2j+1}, \quad (5)$$

where two isolated edge Majorana fermions w_1 and w_{2N} decouple from H as $[H, w_1] = [H, w_{2N}] = 0$, and can be combined to form a Dirac fermion. Since w_1 and w_{2N} are spatially separated, this fermionic excitation is nonlocal and robust to local perturbations, making it an ideal platform to encode a qubit for topological quantum computation. However, the introduction of onsite dissipation ($L_j = -i w_{2j-1} w_{2j}$) destabilizes the aforementioned edge modes.

Throughout the article, we alternatively use the spin representation and Majorana fermion representation to discuss

TABLE I. Definitions of different symbols.

Symbol	Meaning
σ_j^x	Pauli matrices in the Lindblad equation
w_j	Majorana fermions obtained by Jordan-Wigner transformation of Pauli matrices
c_j	Fermion annihilation operators in the LFS
κ_j	Majorana fermions in the LFS (obtained by Jordan-Wigner transformation of c_j)

the problem. We also remind readers that although the specific physical content under these two representations differs greatly (topological edge states can only be discussed in the fermion representation, while the spin representation has no corresponding topological states), mathematically, they can be transformed into each other through Jordan-Wigner transformations.

The density matrix ρ can be expressed as a combination of 4^N Majorana operators

$$w^a := w_1^{a_1} w_2^{a_2} \dots w_{2N}^{a_{2N}}, \quad (6)$$

with $a_j = (0, 1)$. To solve the model in this case, we employ the third quantization formalism proposed by Prosen [42–44,48] and vectorize the density matrix $\rho \rightarrow |\rho\rangle\rangle$, by introducing $w^a \rightarrow |w^a\rangle\rangle$ as the basis vectors of the extended LFS. The master equation can then be recast into a Schrödinger-like equation, namely $i\partial|\rho\rangle\rangle/\partial t = \mathcal{L}|\rho\rangle\rangle$, where the corresponding non-Hermitian Liouvillian reads (see Appendix A for details)

$$\begin{aligned} \mathcal{L} = & -2i \sum_{j=1}^{N-1} J_j [c_{2j}^\dagger c_{2j+1} + c_{2j} c_{2j+1}^\dagger] \\ & + i \sum_{j=1}^N \gamma_j [(2n_{2j-1} - 1)(2n_{2j} - 1) - 1]. \end{aligned} \quad (7)$$

Here c_j and c_j^\dagger are redefined fermion operators in the LFS

$$c_j^\dagger |w^a\rangle\rangle = \delta_{0,a_j} |w_j w^a\rangle\rangle, \quad c_j |w^a\rangle\rangle = \delta_{1,a_j} |w_j w^a\rangle\rangle \quad (8)$$

and satisfy the standard anticommutation relation $\{c_i, c_j^\dagger\} = \delta_{ij}$ and $\{c_i, c_j\} = \{c_i^\dagger, c_j^\dagger\} = 0$.

The equation above represents a dissipative spinless Hubbard model in the extended lattice fermion system, with staggered hoppings and interactions. To facilitate the distinction of different symbols, we list them in detail along with their physical correspondences in Table I. In comparison to the Hermitian case, the lattice size has doubled. The number operator of fermion particles on lattice j is denoted by $n_j = c_j^\dagger c_j$. The explicit forms of applying c_i and c_i^\dagger to the vector $|\rho\rangle\rangle$ can be expressed as follows:

$$(c_{2i-1} + c_{2i-1}^\dagger)|\rho\rangle\rangle \rightarrow \prod_{j<i} \sigma_j^z \sigma_i^x \rho, \quad (9)$$

$$(c_{2i} + c_{2i}^\dagger)|\rho\rangle\rangle \rightarrow \prod_{j<i} \sigma_j^z \sigma_i^y \rho. \quad (10)$$

The presence of local dissipations leads to imaginary nearest-neighbor interactions of $i\gamma_j$ between the nearest lattice pairs $(2j-1, 2j)$. Without loss of generality, we assume $J_j = J$ and $\gamma_j = \gamma$ for all j in the following.

The non-Hermitian Liouvillian \mathcal{L} has an internal symmetry, which significantly simplifies the model. For each

$$P_j = (2n_{2j} - 1)(2n_{2j+1} - 1), \quad (11)$$

with $j = (1, 2, \dots, N-1)$, it is easy to check that

$$[P_j, \mathcal{L}] = 0, \quad [P_j, P_k] = 0. \quad (12)$$

As a result, the right eigenvectors of \mathcal{L} can be chosen as the common eigenvectors of all P_j . Since $P_j^2 = I$, the corresponding eigenvalues P_j can only be $+1$ or -1 . The entire LFS can then be divided into different subspaces labeled by the list $\{p\} = \{P_1, P_2, \dots, P_{N-1}\}$ with $(N-1)$ entries. Since there are 2^{N-1} different lists, the dimension of each subspace is 2×2^N . Therefore, solving the eigensystem of \mathcal{L} is reduced to finding all the eigenvectors of \mathcal{L} within each subspace, which greatly simplifies the computation.

III. EFFECTIVE NON-HERMITIAN KITAEV CHAINS IN LFS

To illustrate the system's hidden topological features, we utilize two cascaded Jordan-Wigner transformations defined as (see Appendix A for further details)

$$\text{JW-I: } \begin{cases} c_{2i-1}^\dagger = \frac{1}{2} \prod_{j=1}^{2i-2} Z_j (X_{2i-1} - iY_{2i-1}), \\ c_{2i}^\dagger = \frac{1}{2} \prod_{j=1}^{2i-1} Z_j (Y_{2i} - iX_{2i}); \end{cases} \quad (13)$$

$$\text{JW-II: } \begin{cases} \kappa_{2i-1} = -\prod_{j=1}^{i-1} X_j Z_i, \\ \kappa_{2i} = \prod_{j=1}^{i-1} X_j Y_i. \end{cases} \quad (14)$$

Here $\{X_k, Y_k, Z_k\}$ are the intermediate local Pauli matrices defined in LFS at site k , and we also introduce a set of $4N$ Liouville-Majorana fermions in the LFS, denoted by κ_k with $k = 1, \dots, 4N$. This allows us to rephrase the Liouvillian operator \mathcal{L} as follows:

$$\mathcal{L} = \sum_j^{N-1} iJ(P_j - 1)\kappa_{4j-1}\kappa_{4j+2} + i\gamma \sum_j^N (i\kappa_{4j-2}\kappa_{4j-1} - 1). \quad (15)$$

To make the above deduction process easier to understand, we illustrate the basic procedure of the transformations in Eqs. (1) to (15), as shown in Fig. 1.

Equation (15) represents one of the main results of the current work. It is easy to verify that within each Liouville subspace defined by $\{P_j = i\kappa_{4j}\kappa_{4j+1}\}$, the effective Liouvillian \mathcal{L} takes the form of a non-Hermitian Kitaev chain with site-dependent couplings $J(P_j - 1)$ ($2J$ or 0) and dissipation rate $i\gamma$. Although it remains challenging to analytically diagonalize $\mathcal{L}_{\{p\}}$ for given $\{P_j\}$, the effective coupling $J_j(P_j - 1)$ vanishes when $P_j = 1$, indicating that the chain is broken at these sites. As a result, the model can be simplified by diagonalizing $\mathcal{L}_{\{p\}}$ within each subchain. In particular, in the subspace defined by $P_j = 1$ for $1 \leq j \leq N-1$, the effective

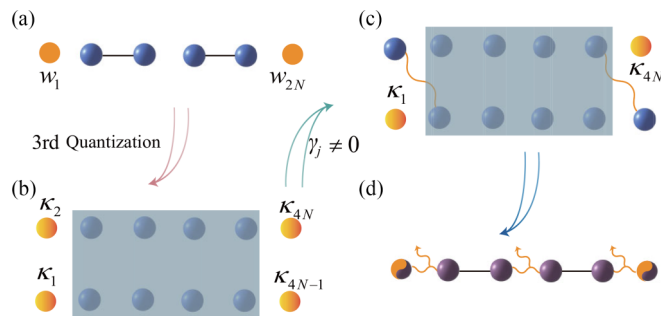


FIG. 1. The diagrammatic representation of Majorana fermions and Liouville-Majorana fermions based on third quantization. In (a) \rightarrow (b), the Liouvillian of the system is obtained in the extended Liouville-Fock space, where two isolated Hermitian Majorana fermions correspond to four isolated Liouville-Majorana fermions. However, due to dissipations with $\gamma \neq 0$, two of these Liouville-Majorana fermions couple to the bulk modes, leaving only two isolated Liouville-Majorana fermions, namely, κ_1 and κ_{4N} , in the system, as shown in (b) \rightarrow (c). Upon mapping back to the original Hilbert space, a Liouville-Majorana fermion can be viewed as a “half-Majorana fermion,” as shown in (c) \rightarrow (d).

Liouvillian can be written as

$$\mathcal{L}_{\{p_j=1\}} = \sum_{j=1}^N i\gamma_j (i\kappa_{4j-2}\kappa_{4j-1} - 1). \quad (16)$$

This describes a series of isolated dissipative coupled pairs of Liouville-Majorana operators. The stationary states of the whole system can also be found in this subspace and satisfies $i\kappa_{4j-2}\kappa_{4j-1}|\rho_s\rangle = |\rho_s\rangle$. Their general form can be written as $\rho_s = (I + \zeta \mathcal{M})/2^N$ with $-1 \leq \zeta \leq 1$ and

$$\mathcal{M} = (-1)^N \prod_{j=1}^N \sigma_j^z. \quad (17)$$

To illustrate the topological features in this model, in Fig. 2, we also provide a diagrammatic representation of the reduced non-Hermitian Kitaev chain in LFS.

IV. LMEMs FOR OPEN BOUNDARIES

For finite lattice, the system supports topological LMEMs in the extended LFS. Specifically, the two Liouville-Majorana modes κ_1 and κ_{4N} are decoupled from \mathcal{L} as

$$[\mathcal{L}, \kappa_1] = [\mathcal{L}, \kappa_{4N}] = 0. \quad (18)$$

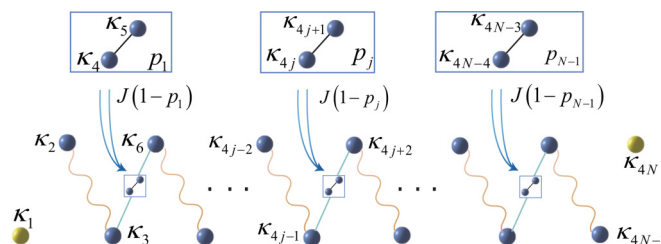


FIG. 2. The reduced non-Hermitian Kitaev chain within the Liouville-Fock subspace defined by $\{p_1, p_2, \dots, p_{N-1}\}$. For specific given $\{p\}$, this chain is broken at the lattice site satisfying $p_j = 1$, and becomes an assembly of subchains with shorter length.

Therefore, we can introduce new Liouville fermionic operators in this subspace \mathcal{H}_e defined by

$$d_e = \frac{1}{2}(\kappa_1 + i\kappa_{4N}), \quad d_e^\dagger = \frac{1}{2}(\kappa_1 - i\kappa_{4N}), \quad (19)$$

with the corresponding number states $|0\rangle\rangle$ and $|1\rangle\rangle$ satisfying $d_e^\dagger d_e |0\rangle\rangle = 0$ and $d_e^\dagger d_e |1\rangle\rangle = |1\rangle\rangle$. This allows us to express the whole LFS $\mathcal{H}_{\mathcal{L}}$ as the tensor-product of the two Liouville-Fock subspaces $\mathcal{H}'_{\mathcal{L}} \otimes \mathcal{H}_e$, where $\mathcal{H}'_{\mathcal{L}}$ denotes the Liouville-Fock subspace expanded by other $(2N - 1)$ Liouville fermionic operators defined by the remaining $(4N - 2)$ Liouville-Majorana modes κ_j with $j = 2, \dots, (4N - 1)$. In Appendix C, we have provided the explicit method to obtain the corresponding vectorized forms of N -site Pauli operators \hat{O}_μ (in the original spin basis) in the extended LFS $\mathcal{H}_{\mathcal{L}}$, where \hat{O}_μ is defined as

$$\hat{O}_\mu = \sigma_1^{\mu_1} \otimes \sigma_2^{\mu_2} \otimes \dots \otimes \sigma_N^{\mu_N}, \quad (20)$$

with $\mu_i \in \{0, x, y, z\}$ and $\sigma^0 = I$ the usual identity matrix. Furthermore, since ρ can always be expanded as the combination of N -site Pauli operators, a general state vector $|\rho\rangle\rangle$ in LFS can then be rewritten as

$$|\rho\rangle\rangle = |\rho'_1\rangle\rangle \otimes |1\rangle\rangle + |\rho'_0\rangle\rangle \otimes |0\rangle\rangle, \quad (21)$$

where $|\rho'_1\rangle\rangle$ and $|\rho'_0\rangle\rangle$ represent the corresponding vectors in $\mathcal{H}'_{\mathcal{L}}$. For an initial product state (see Appendices C and D for the detailed constructions)

$$|\rho(0)\rangle\rangle = |\rho'\rangle\rangle \otimes (a|1\rangle\rangle + b|0\rangle\rangle), \quad (22)$$

since the edge modes are decoupled from the system, $|\rho(t)\rangle\rangle$ remains unentangled during the evolution as

$$|\rho(t)\rangle\rangle = [\exp(-i\mathcal{L}t)|\rho'(0)\rangle\rangle] \otimes (a|1\rangle\rangle + b|0\rangle\rangle). \quad (23)$$

This allows us to find appropriately selected physical observables to verify the existence of the edge modes, as will be discussed in latter sections. We note that the stationary states ρ_s of the whole system also take the product form with $a \sim 1 + \xi$ and $b \sim -(1 - \xi)$, which is consistent with the dynamics analysis mentioned above.

We emphasize that the LMEMs we discuss in this paper are fundamentally different from the conventional Majorana modes found in Hermitian Kitaev chains. Specifically, while the conventional Majorana edge modes are defined within the original Hilbert space, LMEMs are instead defined in the extended LFS. This key difference allows LMEMs to survive for longer periods of time, as opposed to the usual Hermitian Majorana modes which are unstable and decay rapidly in the presence of dissipations.

In a Hermitian system, the existence of topological Majorana modes allows for the definition of a two-dimensional Hilbert space that can support both qubit pure and mixed states. However, in a dissipative system, even though the presence of LMEMs enables the definition of a Hilbert space within the LFS, this does not necessarily imply the existence of a well-defined qubit subspace in the original Hilbert space defined by H . As a result, general LMEMs can only be described as mixed states, which thus motivate us to explore the nontrivial topological features in dissipative systems based on mixed states.

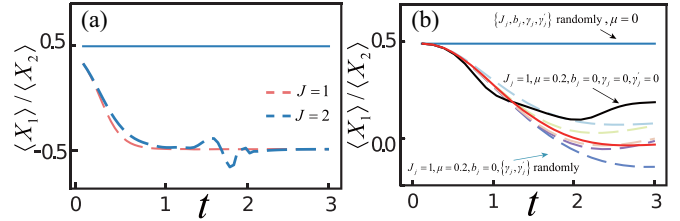


FIG. 3. (a) The evolution of the ratio $\langle X_1 \rangle / \langle X_2 \rangle$ for an initial bulk-edge product states ρ_0 (solid line) and nonproduct states $\tilde{\rho}_0$ (dashed lines) respectively. In the latter case, two different homogeneous couplings with $J = 1$ and $J = 2$ are considered. (b) This figure shows the robustness of LMEMs in the presence of different noises discussed in Eq. (32). The solid blue line shows the robustness of $\langle X_1 \rangle / \langle X_2 \rangle$ against symmetry-preserving perturbations in Eq. (32) with randomized couplings $\{J_j, b_j, \gamma_j, \gamma'_j\}$ when $\mu = 0$. We have computed numerous cases for distinct values of $\{J_j, b_j, \gamma_j, \gamma'_j\}$, all of which coincidentally align along the same curve. For $\mu \neq 0$, $\langle X_1 \rangle / \langle X_2 \rangle$ becomes time-dependent, as shown by solid black and red lines with fixed $\{J_j = 1, \mu = 0.2, b_j = 0\}$ and different decay rates $\{\gamma_j, \gamma'_j\}$. Here, the black line represents the case without any dissipation $\gamma_j = \gamma'_j = 0$. The red line represents the result obtained by calculating the evolution of $\langle X_1 \rangle / \langle X_2 \rangle$ 200 times and taking the average when the dissipation coefficients γ_j and γ'_j are randomly distributed between 0 and 1. All dashed lines represent the time evolution of $\langle X_1 \rangle / \langle X_2 \rangle$ under some specific randomly chosen values of $\{\gamma_j, \gamma'_j\}$. In both figures, we also fix the lattice size to $N = 8$.

Finally, it should be noted that the correlation of LMEMs defined in the LFS does not correspond directly to a measurable observable

$$\langle\langle \rho | i\kappa_1 \kappa_{4N} | \rho \rangle\rangle = \text{tr}(\rho \mathcal{M} \sigma_1^x \sigma_N^x \rho \sigma_1^x \sigma_N^x). \quad (24)$$

This correlation can always be expressed as a quadratic form by suitably chosen observables, as we will demonstrate in the subsequent discussions.

V. DETECTION OF TOPOLOGICALLY PROTECTED LMEMs

The existence of LMEMs can be demonstrated by considering an initial product state $|\rho(0)\rangle\rangle$ as defined in Eq. (22). To illustrate this novel property, we select two Hermitian operators X_1, X_2 that satisfy $|X_1\rangle\rangle = |X'\rangle\rangle \otimes |\phi_1\rangle\rangle$ and $|X_2\rangle\rangle = |X'\rangle\rangle \otimes |\phi_2\rangle\rangle$, namely, $|X_1\rangle\rangle$ and $|X_2\rangle\rangle$ are product vectors in the LFS, and $|\phi_i\rangle\rangle$ is the corresponding state vector in \mathcal{H}_e . In Appendices C and D, we provide a detailed construction method for these operators ρ, X_1, X_2 in the original spin basis. Then using the identity

$$\begin{aligned} \frac{\langle X_1 \rangle}{\langle X_2 \rangle} &= \frac{\text{Tr}(X_1 \rho)}{\text{Tr}(X_2 \rho)} \\ &= \frac{\langle\langle X_1 | \rho \rangle\rangle}{\langle\langle X_2 | \rho \rangle\rangle} \\ &= \frac{\langle\langle \phi_1 | (a|1\rangle\rangle + b|0\rangle\rangle \rangle\rangle}{\langle\langle \phi_2 | (a|1\rangle\rangle + b|0\rangle\rangle \rangle\rangle}, \end{aligned} \quad (25)$$

we conclude that the ratio $\langle X_1 \rangle / \langle X_2 \rangle$ is time-independent and determined solely by the edge modes. However, if the edge modes are coupled with the bulk modes, or the initial state is entangled in the LFS, then $\langle X_1 \rangle / \langle X_2 \rangle$ become time-dependent

and approach a stable value only in the long-time limit as $\rho(\infty) = \rho_s$ is also a product vector.

Figure 3 shows the evolution of the ratio defined in Eq. (25) for different initial states. Here the initial bulk-edge product state ρ_0 and its vectorized form for even N reads

$$\rho_0 = \left[I + \sum_{j=2}^{N-1} 0.2(\sigma_j^x \sigma_{j+1}^x + \sigma_j^z) \right] (I + 0.5\mathcal{M})/2^N \rightarrow |\rho'_0\rangle \otimes (|3|1\rangle - |0\rangle)/\sqrt{10}, \quad (26)$$

where $|\rho'_0\rangle = A(|I_+\rangle + 0.2 \sum_{j=2}^{N-1} |(\sigma_j^x \sigma_{j+1}^x + \sigma_j^z)_+\rangle)$, A is normalization constant, and the operator with $(\dots)_+$ represents the operator in $\mathcal{H}'_{\mathcal{L}}$ after vectorization. The two observables in the spin basis can be chosen as

$$X_1 = \sum_{j=2}^{N-1} (\sigma_j^x \sigma_{j+1}^x + \sigma_j^z) \mathcal{M} \rightarrow |X'\rangle \otimes (|1\rangle + |0\rangle) = |X_1\rangle, \quad (27)$$

$$X_2 = \sum_{j=2}^{N-1} (\sigma_j^x \sigma_{j+1}^x + \sigma_j^z) \rightarrow |X'\rangle \otimes (|1\rangle - |0\rangle) = |X_2\rangle, \quad (28)$$

where $|X'\rangle = A \sum_{j=2}^{N-1} |(\sigma_j^x \sigma_{j+1}^x + \sigma_j^z)_+\rangle$ with A the normalization constant. The numerical calculation shows that

$$\begin{aligned} \frac{\langle X_1 \rangle_t}{\langle X_2 \rangle_t} &= \frac{\langle \langle \rho'_0 | e^{i\mathcal{L}t} | X' \rangle \rangle * (3\langle |1\rangle - \langle |0\rangle \rangle (|1\rangle + |0\rangle))}{\langle \langle \rho'_0 | e^{i\mathcal{L}t} | X' \rangle \rangle * (3\langle |1\rangle - \langle |0\rangle \rangle (|1\rangle - |0\rangle))} \\ &= \frac{3\langle |1\rangle - \langle |0\rangle \rangle (|1\rangle + |0\rangle)}{3\langle |1\rangle - \langle |0\rangle \rangle (|1\rangle - |0\rangle)} \\ &= \frac{\langle X_1 \rangle_0}{\langle X_2 \rangle_0} \end{aligned} \quad (29)$$

is fixed during the evolution, as depicted by the solid line in Fig. 3(a). However, for a nonproduct initial state $\tilde{\rho}_0$ with the vectorized form

$$\begin{aligned} \tilde{\rho}_0 &= \left[\left(I + \sum_{j=2}^{N-1} 0.1 \sigma_j^x \sigma_{j+1}^x \right) (I - 0.5\mathcal{M}) \right. \\ &\quad \left. + \sum_{j=2}^{N-1} 0.2 \sigma_j^z (I + 0.5\mathcal{M}) \right] / 2^N \\ &\rightarrow |X'\rangle \otimes (|1\rangle - |3|0\rangle) + |X''\rangle \otimes (|3|1\rangle - |0\rangle), \end{aligned} \quad (30)$$

where $X' = A'[I_+ + \sum_{j=2}^{N-1} 0.1(\sigma_j^x \sigma_{j+1}^x)_+]$ and $X'' = A'' \sum_{j=2}^{N-1} (\sigma_j^z)_+$ with A' and A'' the relevant normalization constants (see Appendix D for details). The dashed lines in Fig. 3(a) show that the ratio $\langle X_1 \rangle_t / \langle X_2 \rangle_t$ changes with time, indicating the entanglement between the edge and bulk modes in this case.

The edge modes are topologically protected by the internal symmetry in LFS. For any perturbations characterized by introducing additional Hamiltonian H' or dissipators L'_j into the Lindblad equation, the edge modes become decoupled from the bulk modes as long as the corresponding Lindbladians in the LFS commute with κ_1 and κ_{4N} . Using spin language, we

can choose these operators such that

$$[H'(L'), \sigma_1^x] = [H'(L'), \sigma_N^x] = \left[H'(L'), \prod_{j=1}^N \sigma_j^z \right] = 0. \quad (31)$$

For comparative purposes, in Fig. 3(b), we also plot the evolution of $\langle X_1 \rangle / \langle X_2 \rangle$ for Lindblad equation with

$$H = \sum_{j=1}^{N-1} J_j \sigma_j^x \sigma_{j+1}^x + \sum_{j=2}^{N-1} b_j \sigma_j^z + \mu \sum_{j=1}^N \sigma_j^x. \quad (32)$$

The two different types of dissipators are $L_j = \sqrt{\gamma_j} \sigma_j^z$ ($j = 1, \dots, N$) and $L'_j = \sqrt{\gamma'_j} \sigma_j^x \sigma_{j+1}^x$ ($j = 1, \dots, N-1$). For the initial bulk-edge product state ρ_0 shown in Eq. (26), our calculations show that $\langle X_1 \rangle / \langle X_2 \rangle$ remains fixed for all coefficients $\{J_j, b_j, \gamma_j, \gamma'_j\}$ randomly distributed between 0 and 1 when $\mu = 0$. Here L_j, L'_j and $\sum_{j=2}^{N-1} b_j \sigma_j^z$ satisfy the constraints of Eq. (31). Thus, the presence of local random magnetic fields or other random special dissipators will not disrupt the edge states, which signifies the topological feature of the LMEMs.

For nonzero $\mu \neq 0$, since $\sum_{j=1}^N \sigma_j^x$ does not satisfy Eq. (31), the edge modes becomes unstable in this case. Correspondingly, $\langle X_1 \rangle / \langle X_2 \rangle$ changes during the evolution as the edge modes couple to the bulk due to the perturbations, which indicates the failure of topological protection in the system.

VI. PURITY AS THE DETECTION OF LONG-RANGE CORRELATION IN LFS

The initial state $|\rho(0)\rangle$ described in Eq. (22) can also be used to examine the correlation defined by $\langle \langle \rho | i\kappa_1 \kappa_{4N} | \rho \rangle \rangle$. Since $i\kappa_1 \kappa_{4N} | \rho \rangle \rangle = |\rho'\rangle \otimes (a|1\rangle - b|0\rangle)$, the correlation can be simplified as

$$\langle \langle \rho | i\kappa_1 \kappa_{4N} | \rho \rangle \rangle = \frac{|a|^2 - |b|^2}{|a|^2 + |b|^2} \langle \langle \rho | \rho \rangle \rangle \propto \text{Tr}(\rho^2), \quad (33)$$

where $\text{Tr}(\rho^2) = \langle \langle \rho | \rho \rangle \rangle$ is the purity of the state ρ . After inserting the completeness relation in LFS, we have

$$\langle \langle \rho | \rho \rangle \rangle = \sum_{\mu} \frac{\langle \langle \rho | \hat{O}_{\mu} \rangle \rangle \langle \langle \hat{O}_{\mu} | \rho \rangle \rangle}{2^N} = \sum_{\mu} \frac{|\langle \hat{O}_{\mu} \rangle|^2}{2^N}, \quad (34)$$

where \hat{O}_{μ} are the usual N -site Pauli operators (see Appendix E for details). The correlation $\langle \langle \rho | i\kappa_1 \kappa_{4N} | \rho \rangle \rangle$ can then be expressed as a quadratic form of observables defined by \hat{O}_{μ} . For dissipative systems, the dynamics in the long-time limit can be expressed as

$$|\rho(t)\rangle = \sum_j e^{-i\lambda_j t} |\rho'_j\rangle \otimes (a|1\rangle + b|0\rangle), \quad (35)$$

which is mainly determined by eigenvectors $|\rho'_j\rangle$ with minimal $|\text{Im}(\lambda_j)|$ such that $\mathcal{L}|\rho'_j\rangle = \lambda_j |\rho'_j\rangle$ and $\text{Im}(\lambda_j) \leq 0$. This indicates that the summation in Eq. (34) can be well approximated by choosing a subset \hat{O}_m ($m = 1, \dots, M$) with much fewer observables ($M \ll N$), thereby simplifying the detection in experiments.

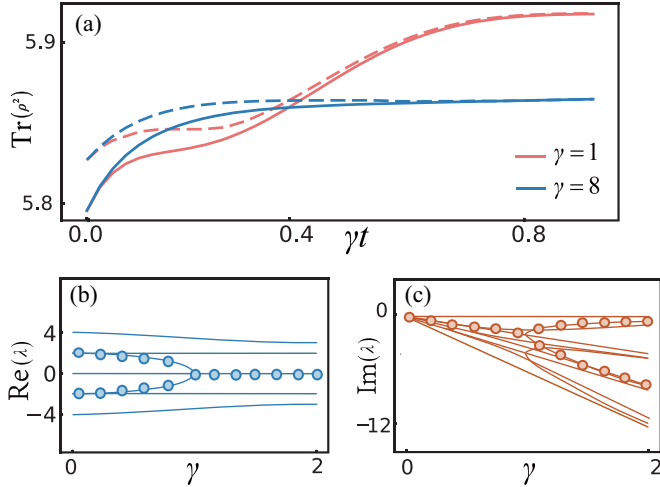


FIG. 4. (a) The evolution of $\text{Tr}(\rho^2)$ for an initial bulk-edge product state with lattice size $N = 8$. The dotted line is the approximated purity obtained by Eq. (37), which is compared with the precise values obtained by solving the Lindblad equation directly (solid line). The two results match well for larger γt . Panels (b) and (c) are the real and imaginary parts of Liouville spectrum for $(N=6, J=2)$. The circles are the eigenvalues within the subspace defined by $\{P_{j \neq 1} = 1(\forall j), P_1 = -1\}$.

In Fig. 4, we present the time evolution of $\langle\langle \rho(t) | \rho(t) \rangle\rangle$ for the initial product state

$$\begin{aligned} \rho(0) &= I + 0.3\mathcal{M}(\sigma_1^z + \sigma_1^y \sigma_2^x + \sigma_1^y \sigma_3^x + \sigma_2^z \sigma_2^x \sigma_3^x) / 2^N \\ &\rightarrow |X'\rangle \otimes (|1\rangle - |0\rangle), \end{aligned} \quad (36)$$

where $X' = A(I_+ - 0.3(\sigma_1^z + \sigma_1^y \sigma_2^x + \sigma_1^y \sigma_3^x + \sigma_2^z \sigma_2^x \sigma_3^x)_+)$ with A the normalization constant. This state has nonzero components in subspaces defined by $P_j = 1(\forall j)$ and $P_{j \neq 1} = 1(\forall j), P_1 = -1$. As we increase the dissipation rate γ , the Lindblad spectra λ_j exhibit exceptional points, as illustrated in Figs. 4(b) and 4(c). In addition, the system supports numerous quasi-stable states with $\text{Im}(\lambda) \rightarrow 0^-$ as $\gamma \rightarrow \infty$. The correlation $\langle\langle \rho | i\kappa_1 \kappa_{4N} | \rho \rangle\rangle$ can be approximated as

$$\langle\langle \rho | i\kappa_1 \kappa_{4N} | \rho \rangle\rangle \sim (1 + \langle \sigma_1^y \sigma_2^x \rangle^2 + \langle \sigma_1^z \rangle^2). \quad (37)$$

Hence, to obtain the long-time evolution of $\text{Tr}(\rho^2)$, we can rely on detecting only short-range correlations defined by $\langle \sigma_1^y \sigma_2^x \rangle$ and $\langle \sigma_1^z \rangle$. When the decay rate γ is large, the obtained result fits well with the exact result, as shown in Fig. 4(a) by the dashed line.

VII. DISCUSSION AND CONCLUSION

To summarize, we have investigated an exactly solvable model of an open system described by Lindblad master equations and discovered a novel type of topologically protected Liouville-Majorana mode hidden within the Liouvillian. Specifically, we demonstrate that the mode generally corresponds to mixed states of the system, a feature that differs from Hermitian systems, where it can be described in terms of pure states. Remarkably, this mode is found to be robust and stable throughout the entire dynamic process,

contrasting with the stationary state of the Liouville equation. Our findings pave the way for further exploration of nontrivial topological states defined in the extended LFS and expand the investigation of topological physics for mixed states in dissipative systems.

ACKNOWLEDGMENTS

We thank Prof. X.-W. Luo for helpful discussions. This work was funded by National Natural Science Foundation of China (Grants No. 11974334 and No. 11774332), and Innovation Program for Quantum Science and Technology (Grant No. 2021ZD0301200). X.F.Z. also acknowledges support from CAS Project for Young Scientists in Basic Research (Grant No. YSBR-049).

APPENDIX A: NON-HERMITIAN EFFECTIVE LIOUVILLIAN IN THE EXTENDED LIOUVILLE-FOCK SPACE

In this Appendix, we present the explicit derivation of the effective Liouvillian in the extended Liouville Fock space using the third quantization formalism.

For an open system under the Markov approximation, the dynamics of its density matrix ρ are governed by the Lindblad master equation,

$$i \frac{d\rho}{dt} = \hat{\phi}_L[\rho] = [H, \rho] + i \sum_j \left(L_j \rho L_j^\dagger - \frac{1}{2} \{L_j^\dagger L_j, \rho\} \right). \quad (A1)$$

This equation describes the nonunitary time evolution of the system due to interactions with the external environment. The first term represents the unitary dynamics, where H is the system's Hamiltonian. L_j is the corresponding Lindblad operator that characterizes the j th dissipation channel with a decay rate γ_j .

By treating ρ as a vector $|\rho\rangle\rangle$ and considering the linearity of the system, we can rewrite the equation as

$$i \frac{d|\rho\rangle\rangle}{dt} = \mathcal{L}|\rho\rangle\rangle, \quad (A2)$$

which takes a similar form to the conventional Schrödinger equation, with the effective non-Hermitian Liouvillian \mathcal{L} . The explicit form of \mathcal{L} depends on how we vectorize the matrix ρ . Specifically, for a quadratic spin/Fermi system, the process of vectorization can be easily discussed using the Majorana representation. Notably, Prosen introduced the third quantization formalism in Refs. [42–44], which provides an elegant and systematic approach to solving this dissipative system.

For a 1D system of N spins/Fermions, the density matrix can be expressed in terms of Majorana operators as

$$\rho = \frac{1}{2^{2N}} \sum_{a_1, \dots, a_{2N}} c_{a_1, a_2, a_3, \dots, a_{2N}} w_1^{a_1} w_2^{a_2} w_3^{a_3} \dots w_{2N}^{a_{2N}}, \quad (A3)$$

where w_j represents the Majorana operators that satisfy the anticommutation relation $\{w_j, w_k\} = 2\delta_{jk}$. The variable a_j corresponds to the excitation number of the w_j operator and can take values of either 0 or 1. The coefficients $c_{a_1, a_2, a_3, \dots, a_{2N}}$ are real numbers. Notably, for the spin-1/2 system discussed in the main text, this representation is always possible thanks

to the Jordan-Wigner transformation. The Pauli matrices σ_j^x and σ_j^y can be expressed in terms of Majorana operators as

$$\sigma_j^x = \prod_{k < j} (-i w_{2k-1} w_{2k}) w_{2j-1}, \quad (\text{A4})$$

$$\sigma_j^y = \prod_{k < j} (-i w_{2k-1} w_{2k}) w_{2j}. \quad (\text{A5})$$

For later convenience, we introduce the following definition:

$$w^a := w_1^{a_1} w_2^{a_2} \dots w_{2N}^{a_{2N}}, \quad (\text{A6})$$

where n_a represents the total count of Majorana operators in the basis vector $|w^a\rangle$ and is given by the sum over index j as $n_a := \sum_j a_j$. To perform vectorization of the master equation, we associate the Hilbert space $\mathcal{H}_{\mathcal{L}}$ with the defined basis given by

$$|w^a\rangle := |w_1^{a_1} w_2^{a_2} \dots w_{2N}^{a_{2N}}\rangle. \quad (\text{A7})$$

In this context, we consider the 4^n -dimensional space of operators denoted as w^a . Importantly, the Hamiltonian and relevant Lindbladians can also be expressed as combinations of Majorana operators w^a . Consequently, the Liouville superoperator \mathcal{L} can be represented as an operator within this newly defined Liouville-Fock space (LFS). Specifically, for each Majorana operator w_k that appears in H or L_i and acts on the basis $|w^a\rangle$, we can introduce fermionic operators c_j and c_j^\dagger , defined as

$$c_j^\dagger |w_1^{a_1} w_2^{a_2} \dots w_{2N}^{a_{2N}}\rangle = \delta_{0,a_j} |w_j w_1^{a_1} w_2^{a_2} \dots w_{2N}^{a_{2N}}\rangle, \quad (\text{A8})$$

$$c_j |w_1^{a_1} w_2^{a_2} \dots w_{2N}^{a_{2N}}\rangle = \delta_{1,a_j} |w_j w_1^{a_1} w_2^{a_2} \dots w_{2N}^{a_{2N}}\rangle, \quad (\text{A9})$$

where the fermionic operators satisfy the standard canonical anticommutation relations

$$\{c_j, c_k\} = 0, \quad \{c_j, c_k^\dagger\} = \delta_{jk}, \quad \{c_j^\dagger, c_k^\dagger\} = 0. \quad (\text{A10})$$

For an N -site spin/fermionic system, the dimension of the Fock space $\mathcal{H}_{\mathcal{L}}$ is 4^N . Therefore, we have $2N$ fermionic operators, denoted as c_j with $j = (1, 2, \dots, 2N)$.

The master equation of the system can be expressed using Majorana operators as follows:

$$\begin{aligned} i|\dot{\rho}\rangle\rangle &= -i \sum_{j=1}^{N-1} J_j (w_{2j} w_{2j+1} \rho - \rho w_{2j} w_{2j+1}) \\ &+ i \sum_{j=1}^N \gamma_j (w_{2j-1} w_{2j} \rho w_{2j} w_{2j-1} - \rho). \end{aligned} \quad (\text{A11})$$

Based on the preceding discussions, it can be verified that when mapped into the LFS, operators acting on ρ can be redefined using fermionic operators

$$\omega_j \rho \implies (c_j + c_j^\dagger) |\rho\rangle\rangle, \quad (\text{A12})$$

$$\rho \omega_i \implies (c_j - c_j^\dagger) (c_j - c_j^\dagger) |\rho\rangle\rangle. \quad (\text{A13})$$

By employing these substitutions, we can readily obtain the corresponding Liouvillian \mathcal{L} , which can be expressed as

$$\begin{aligned} \mathcal{L} &= -2i \sum_{j=1}^{N-1} J_j (c_{2j}^\dagger c_{2j+1} + c_{2j} c_{2j+1}^\dagger) \\ &- i \sum_{j=1}^N \gamma_j + i \sum_{j=1}^N \gamma_j (2n_{2j-1} - 1)(2n_{2j} - 1), \end{aligned} \quad (\text{A14})$$

where $n_j = c_j^\dagger c_j$ is the number operator on site j . Since \mathcal{L} commutes with all $P_j = (2n_{2j} - 1)(2n_{2j+1} - 1)$ for $j = (1, 2, \dots, N-1)$, and $P_j^2 = I$, the right eigenvectors of \mathcal{L} can be chosen as the common eigenvectors of all P_j . The corresponding eigenvalues p_j can only be $+1$ or -1 . Consequently, the entire LFS can be divided into different subspaces, which are labeled by the list $\{p\} = \{p_1, p_2, \dots, p_{N-1}\}$ with $(N-1)$ entries.

To obtain the effective interactions of \mathcal{L} , we introduce another set of Jordan-Wigner transformations (JW-I) defined as $c_{2i-1}^\dagger = \frac{1}{2} \prod_{j=1}^{2i-2} Z_j (X_{2i-1} - iY_{2i-1})$ and $c_{2i}^\dagger = \frac{1}{2} \prod_{j=1}^{2i-1} Z_j (Y_{2i} - iX_{2i})$. After employing these transformations, we can map the system into an effective spin model, defined as follows:

$$\mathcal{L} = \sum_j^{N-1} J(P_j - 1) Y_{2j} Y_{2j+1} - i\gamma \sum_i (Z_{2j-1} Z_{2j} + 1). \quad (\text{A15})$$

Here, $\{X_k, Y_k, Z_k\}$ are the local Pauli matrices defined in the LFS at site k . We have also set the homogeneous decay rates as $\gamma_j = \gamma$. Therefore, within each subblock denoted by $\{p\}$, \mathcal{L} takes the form of a non-Hermitian spin model with site-dependent couplings $J(p_j - 1)$ and a dissipation rate of $i\gamma$.

To illustrate the hidden topological features of the system, we employ another Jordan-Wigner transformation (JW-II) again and define the local Liouville-Majorana operators as $\kappa_{2i-1} = -\prod_{j=1}^{i-1} X_j Z_i$ and $\kappa_{2i} = \prod_{j=1}^{i-1} X_j Y_i$, and finally we arrive at

$$\mathcal{L} = \sum_j^{N-1} iJ(P_j - 1) \kappa_{4j-1} \kappa_{4j+2} + i\gamma \sum_j^N (i\kappa_{4j-2} \kappa_{4j-1} - 1), \quad (\text{A16})$$

with $P_j = i\kappa_{4j} \kappa_{4j+1}$. Therefore, for given $\{p\}$, \mathcal{L} reduces to an effective non-Hermitian Kitaev chain with site-dependent couplings.

We stress that although both ω_j and κ_j are Majorana operators (MOs), they are defined in different spaces. Specifically, ω_j is the MO defined in the original Hilbert space, and κ_j is another type of MO defined in the extended LFS (denoted by $\mathcal{H}_{\mathcal{L}}$ in the paper). For N -site chain, we have $2N$ ω -type MOs, but $4N$ κ -type Liouville-MOs. So generally speaking, one ω -type MO maps to two κ -type MOs. In this sense, we claim that a Liouville-Majorana fermion can be viewed as a half-Majorana fermion in the original Hilbert space. In the spin basis defined in Eq. (1), the Liouville-Majorana edge modes discussed in the paper can only be described as mixed states, which is different from the case for the usual Hermitian Majorana modes.

APPENDIX B: THE SPECTRA AND DYNAMICAL FEATURES OF LIOUVILLIAN \mathcal{L}

To explore the dynamical properties of system, we consider the eigenmatrices and eigenvalues of the Liouville superoperator $\hat{\phi}_L$ and its counterpart \mathcal{L} in the Liouville Fock space \mathcal{H}_L ,

$$\hat{\phi}_L[\rho_m] = \lambda_m \rho_m \rightarrow \mathcal{L}|\rho_m\rangle\rangle = \lambda_m |\rho_m\rangle\rangle. \quad (\text{B1})$$

For a master equation in the Lindblad form, it has been shown that the spectrum $\{\lambda_m\}$ satisfies the following properties which are useful for later discussions.

First, since the imaginary part of λ_m is linked with the dissipation dynamics toward stationary states, we have $\text{Im}[\lambda_m] \leq 0$. The stationary state ρ_s of the system corresponds to the eigenmatrix ρ_0 with $\lambda_0 = 0$. So we have $\rho_s = \rho_0/\text{Tr}[\rho_0]$. Additionally, if stationary states are degenerate, then the system can evolve toward different steady states depending on the initial conditions.

Second, since ρ is Hermitian, and $\hat{\phi}_L[\sigma^\dagger] = -(\hat{\phi}_L[\sigma])^\dagger$ for any matrix σ , the eigenvalues must come in anticongjugate pairs $\{\lambda_m, -\lambda_m^*\}$. Therefore, if λ_m is pure imaginary, then the eigenmatrix ρ_m must be Hermitian and vice versa.

Finally, if $\text{Im}[\lambda_m] \neq 0$, since the Liouvillian evolution is trace-preserving, the eigenmatrix evolves as $e^{-i\lambda_m t} \rho_m \rightarrow 0$ when $t \rightarrow \infty$. This leads to $\text{Tr}[\rho_m] = 0$.

Equipped with the eigensystem of the Lindblad equation, we can then discuss the dynamics of the system in a more convenient manner. Since any physical state of the system can always be decomposed as

$$\rho = g_0 \rho_s + \sum_{m \neq 0} g_m \rho_m, \quad (\text{B2})$$

the time-evolution of $\rho(t)$ in LFS \mathcal{H}_L can then be simplified as

$$|\rho(t)\rangle\rangle = g_0 |\rho_s\rangle\rangle + \sum_{m \neq 0} g_m e^{-i\lambda_m t} |\rho_m(t)\rangle\rangle. \quad (\text{B3})$$

We stress that the dynamical properties of a quantum system with the effective Liouvillian \mathcal{L} is very different from the usual non-Hermitian system solely driven by an effective non-Hermitian Hamiltonian $H_e = H - i\gamma \sum_m L_m^\dagger L_m / 2$. In the later case, the effect of quantum jump $L_m \rho L_m^\dagger$ has been neglected. We also note that the non-Hermiticity of H_e can result in many novel effects. For instance, pseudo-Hermitian or PT-symmetric H_e has been widely discussed in the past decades, which gives rise to rich exotic phenomena in different subjects of physics. However, in many cases, this jump term $L_m \rho L_m^\dagger$ cannot be dropped and can change the dynamical behavior of the system dramatically.

APPENDIX C: BULK-EDGE PRODUCT VECTORS OF PAULI OPERATORS IN LFS

In this Appendix, we show that all the Pauli operators in the original spin basis map to bulk-edge product vectors in LFS. This allows us to construct various initial product vectors and detection operators discussed in the main text.

Specifically, the two edge Liouville-Majorana operators κ_1 and κ_{4N} can be used to define the Dirac fermionic operator $d_e = \frac{1}{2}(\kappa_1 + i\kappa_{4N})$ and $d_e^\dagger = \frac{1}{2}(\kappa_1 - i\kappa_{4N})$. The corresponding

number operator reads $d_e^\dagger d_e$ and satisfies the following properties after acting on its local Fock basis

$$d_e^\dagger d_e |1\rangle\rangle = |1\rangle\rangle, \quad d_e^\dagger d_e |0\rangle\rangle = 0. \quad (\text{C1})$$

Since d_e and d_e^\dagger commute with the Liouvillian \mathcal{L} , $|0\rangle\rangle$ and $|1\rangle\rangle$ correspond to the two local dark modes of the system, and defined as the basis of the local Fock space denoted by \mathcal{H}_e . For the remaining Liouville-Majorana operators κ_j with $2 \leq j \leq (4N - 1)$, they can be combined similarly to define $(2N - 1)$ Dirac fermionic operators with the corresponding Fock space denoted by \mathcal{H}'_L . Therefore, the whole LFS \mathcal{H}_L can then be expressed as the tensor product of \mathcal{H}'_L and \mathcal{H}_e . Using these notations, we can then rewrite the state vector $|\rho\rangle\rangle$ in LFS as

$$|\rho\rangle\rangle = |\psi_1\rangle\rangle|1\rangle\rangle + |\psi_0\rangle\rangle|0\rangle\rangle. \quad (\text{C2})$$

For operators acting on $|\rho\rangle\rangle$ in LFS, they can be mapped to the corresponding linear operations in the original Hilbert space defined by the spin basis. For later convenience, we list the explicit correspondence as follows:

$$d_e^\dagger d_e |\rho\rangle\rangle \rightarrow \frac{1}{2}(\rho + \mathcal{M}\sigma_1^x \sigma_N^x \rho \sigma_1^x \sigma_N^x), \quad (\text{C3})$$

$$d_e |\rho\rangle\rangle \rightarrow \frac{1}{2}\mathcal{M}\sigma_1^x (\mathcal{M}\sigma_1^x \sigma_N^x \rho \sigma_N^x \sigma_1^x + \rho)\mathcal{M}\sigma_1^x, \quad (\text{C4})$$

$$d_e^\dagger |\rho\rangle\rangle \rightarrow -\frac{1}{2}\mathcal{M}\sigma_1^x (\mathcal{M}\sigma_1^x \sigma_N^x \rho \sigma_N^x \sigma_1^x - \rho)\mathcal{M}\sigma_1^x, \quad (\text{C5})$$

where $\mathcal{M} = (-1)^N \prod_{j=1}^N \sigma_j^z$. One can check that if $|\rho\rangle\rangle = |\rho_1\rangle\rangle = |\psi_1\rangle\rangle|1\rangle\rangle$, then we have

$$d_e^\dagger d_e |\rho_1\rangle\rangle = |\rho_1\rangle\rangle \rightarrow \mathcal{M}\sigma_1^x \sigma_N^x \rho_1 \sigma_1^x \sigma_N^x = \rho_1. \quad (\text{C6})$$

Similarly, if $|\rho\rangle\rangle = |\rho_0\rangle\rangle = |\psi_0\rangle\rangle|0\rangle\rangle$, then we have

$$d_e^\dagger d_e |\rho_0\rangle\rangle = |\rho_0\rangle\rangle \rightarrow \mathcal{M}\sigma_1^x \sigma_N^x \rho_0 \sigma_1^x \sigma_N^x = -\rho_0. \quad (\text{C7})$$

This also indicates that if ρ_i is Hermitian, then we must have $[\rho_i, \mathcal{M}] = 0$.

To obtain the explicit form in LFS for a given density matrix, we consider the following N -body Pauli operator in the original Hilbert space $\hat{O} = \sigma_1^{\mu_1} \otimes \sigma_2^{\mu_2} \otimes \cdots \otimes \sigma_N^{\mu_N}$ with $\mu_i \in \{0, x, y, z\}$ and $\sigma^0 = I$ the usual identity matrix. The relevant state vector in LFS reads

$$|\hat{O}\rangle\rangle = |\hat{O}_1\rangle\rangle|1\rangle\rangle + |\hat{O}_0\rangle\rangle|0\rangle\rangle. \quad (\text{C8})$$

To show that $|\hat{O}\rangle\rangle$ can be written as a product state in LFS, we define the following two projectors

$$P_+ = \frac{1}{2}(I + \mathcal{M}), \quad P_- = \frac{1}{2}(I - \mathcal{M}),$$

with $P_\pm^2 = I$. Since \hat{O} is commuted ($\delta_o = +1$) or anticommuted ($\delta_o = -1$) with $\prod_{i=1}^N \sigma_i^z \sigma_1^x \sigma_N^x$ as

$$\hat{O} \prod_{i=1}^N \sigma_i^z \sigma_1^x \sigma_N^x = \delta_o \prod_{i=1}^N \sigma_i^z \sigma_1^x \sigma_N^x \hat{O}, \quad (\text{C9})$$

we have

$$\mathcal{M}\sigma_1^x \sigma_N^x \hat{O} P_\pm \sigma_1^x \sigma_N^x = \delta_o \hat{O} P_\pm \mathcal{M} = \pm \delta_o \hat{O} P_\pm. \quad (\text{C10})$$

Using Eqs. (C6) and (C7), we conclude that $|\hat{O}P_+\rangle\rangle$ and $|\hat{O}P_-\rangle\rangle$ can be written as

$$|\hat{O}P_\pm\rangle\rangle = |\hat{O}_\pm\rangle\rangle \left| \frac{1 \pm \delta_o}{2} \right\rangle, \quad (\text{C11})$$

where $|\hat{O}_\pm\rangle\rangle$ represent the corresponding state vectors in $\mathcal{H}'_{\mathcal{L}}$, whose explicit forms are irrelevant to the latter discussion. Therefore, the vectors related to \hat{O} and $\hat{O}\mathcal{M}$ then read

$$|\hat{O}\rangle\rangle = |\hat{O}_+\rangle\rangle \left| \frac{1+\delta_o}{2} \right\rangle\rangle + |\hat{O}_-\rangle\rangle \left| \frac{1-\delta_o}{2} \right\rangle\rangle, \quad (\text{C12})$$

$$|\hat{O}\mathcal{M}\rangle\rangle = |\hat{O}_+\rangle\rangle \left| \frac{1+\delta_o}{2} \right\rangle\rangle - |\hat{O}_-\rangle\rangle \left| \frac{1-\delta_o}{2} \right\rangle\rangle. \quad (\text{C13})$$

To show that both $|\hat{O}\rangle\rangle$ and $|\hat{O}\mathcal{M}\rangle\rangle$ can be written as product vectors in LFS, we need to show that $|\hat{O}_+\rangle\rangle \propto |\hat{O}_-\rangle\rangle$. This can be achieved by noticing that

$$d_e |\hat{O}P_+\rangle\rangle = \frac{1+\delta_o}{2} |\hat{O}_+\rangle\rangle |0\rangle\rangle, \quad (\text{C14})$$

which is nonzero only when $\delta_o = +1$. The corresponding matrix form in the original Hilbert space reads

$$\begin{aligned} & -\frac{1}{2} \mathcal{M} \sigma_1^x (\mathcal{M} \sigma_1^x \sigma_N^x \hat{O} P_+ \sigma_N^x \sigma_1^x + \hat{O} P_+) \sigma_1^x \mathcal{M} \\ & = -\frac{1+\delta_o}{2} \sigma_N^x \hat{O} P_+ \sigma_N^x \\ & = -\frac{1+\delta_o}{2} \sigma_N^x \hat{O} \sigma_N^x P_-. \end{aligned} \quad (\text{C15})$$

By setting $\delta_o = +1$ and noticing $\sigma_N^x \hat{O} = \gamma_o \sigma_N^x \hat{O}$ with $\gamma_o = \pm 1$, we have

$$|\hat{O}_+\rangle\rangle |0\rangle\rangle = -\gamma_o |\hat{O}_-\rangle\rangle |0\rangle\rangle, \quad (\text{C16})$$

which leads to $|\hat{O}_+\rangle\rangle = -\delta_o \gamma_o |\hat{O}_-\rangle\rangle$.

We note that similar result can also be obtained if we consider

$$d_e^\dagger |\hat{O}P_+\rangle\rangle = \frac{1-\delta_o}{2} |\hat{O}_+\rangle\rangle |1\rangle\rangle, \quad (\text{C17})$$

for $\delta_o = -1$. The corresponding matrix form reads

$$\begin{aligned} & -\frac{1}{2} \mathcal{M} \sigma_1^x (-\mathcal{M} \sigma_1^x \sigma_N^x (\hat{O} + \hat{O}\mathcal{M}) \sigma_N^x \sigma_1^x + \hat{O} + \hat{O}\mathcal{M}) \sigma_1^x \mathcal{M} \\ & = -\frac{\delta_o-1}{2} \sigma_N^x \hat{O} P_+ \sigma_N^x \\ & = -\frac{\delta_o-1}{2} \gamma_o \hat{O} P_-. \end{aligned} \quad (\text{C18})$$

After writing back to the LFS, we again obtain $|\hat{O}_+\rangle\rangle = -\delta_o \gamma_o |\hat{O}_-\rangle\rangle$.

Summing up all the above discussions, we conclude that both $|\hat{O}\rangle\rangle$ and $|\hat{O}\mathcal{M}\rangle\rangle$ are product and read

$$|\hat{O}\rangle\rangle = |\hat{O}_+\rangle\rangle \left[\left| \frac{1+\delta_o}{2} \right\rangle\rangle - \delta_o \gamma_o \left| \frac{1-\delta_o}{2} \right\rangle\rangle \right], \quad (\text{C19})$$

$$|\hat{O}\mathcal{M}\rangle\rangle = |\hat{O}_+\rangle\rangle \left[\left| \frac{1+\delta_o}{2} \right\rangle\rangle + \delta_o \gamma_o \left| \frac{1-\delta_o}{2} \right\rangle\rangle \right], \quad (\text{C20})$$

where other relevant coefficients are defined as follows:

$$\sigma_N^x \hat{O} = \gamma_o \sigma_N^x \hat{O}, \quad (\text{C21})$$

$$\hat{O}\mathcal{M} \sigma_1^x \sigma_N^x = \delta_o \mathcal{M} \sigma_1^x \sigma_N^x \hat{O}. \quad (\text{C22})$$

The above derivation indicates that the 4^N Pauli operators \hat{O}_μ can be divided into 2^{2N-1} different pairs up to a constant phase

factors as $(\hat{O}_\mu, \hat{O}_\mu \mathcal{M})$. For any two different pairs $(\hat{O}_1, \hat{O}_1 \mathcal{M})$ and $(\hat{O}_2, \hat{O}_2 \mathcal{M})$, since

$$\text{tr}(\hat{O}_i \hat{O}_j \mathcal{M}) = 0, \quad \text{tr}(\mathcal{M} \hat{O}_i \hat{O}_j \mathcal{M}) = 2^N \delta_{ij}, \quad (\text{C23})$$

we have

$$\langle\langle \hat{O}_i | \hat{O}_j \rangle\rangle = 2^N \delta_{ij}, \quad \langle\langle \hat{O}_{i,+} | \hat{O}_{j,+} \rangle\rangle = 2^{N-1} \delta_{ij}. \quad (\text{C24})$$

Given the state vector in LFS shown as Eq. (C8), we also can easily obtain the matrix form in the original spin basis using the following maps:

$$\delta_o = +1: \begin{cases} |\hat{O}_+\rangle\rangle |1\rangle\rangle \rightarrow \hat{O} P_+, \\ |\hat{O}_+\rangle\rangle |0\rangle\rangle \rightarrow -\gamma_o |\hat{O}_-\rangle\rangle |0\rangle\rangle = -\gamma_o \hat{O} P_-, \end{cases} \quad (\text{C25})$$

$$\delta_o = -1: \begin{cases} |\hat{O}_+\rangle\rangle |0\rangle\rangle \rightarrow \hat{O} P_+, \\ |\hat{O}_+\rangle\rangle |1\rangle\rangle \rightarrow \gamma_o |\hat{O}_-\rangle\rangle |0\rangle\rangle = \gamma_o \hat{O} P_-. \end{cases} \quad (\text{C26})$$

APPENDIX D: CONSTRUCTING BULK-EDGE PRODUCT STATES IN LFS AND THE ORIGINAL SPIN BASIS

In this Appendix, we provide how bulk-edge product vectors in LFS can be obtained using pairs of Pauli operators. The robustness of edge modes and their internal symmetry can be also easily discussed based on these constructions.

For the system consider in the main text, the general form of the stationary states ρ_s can be written as the combination of Pauli operators $(\hat{O}, \hat{O}\mathcal{M})$ with $\hat{O} = I$ and $\delta_o = \gamma_o = 1$. This means

$$\rho_s = \frac{1}{2^N} (I + \zeta \mathcal{M}) = \frac{1}{2^N} [(1 + \zeta) I P_+ + (1 - \zeta) I P_-], \quad (\text{D1})$$

where ζ is real and satisfies $|\zeta| \leq 1$ to ensure the positivity of ρ_s . The corresponding vectorized form in LFS reads

$$|\rho_s\rangle\rangle = \frac{1}{2^N} |I_+\rangle\rangle [(1 + \zeta) |1\rangle\rangle - (1 - \zeta) |0\rangle\rangle]. \quad (\text{D2})$$

For a given initial state vector $|\rho(t=0)\rangle\rangle$ in LFS, if $|\rho(t=0)\rangle\rangle = |\rho'\rangle\rangle \otimes (a|1\rangle\rangle + b|0\rangle\rangle)$ is product, then $|\rho(t)\rangle\rangle$ remains unentangled in LFS under time evolution. Since the system tends to its stationary state defined by Eq. (D2) in the long-time limit, we conclude that the product state can always be rewritten as

$$|\rho\rangle\rangle = |\rho_+\rangle\rangle \otimes [(1 + \zeta) |1\rangle\rangle - (1 - \zeta) |0\rangle\rangle] / 2^N, \quad (\text{D3})$$

where the most general form of $|\rho_+\rangle\rangle$ reads

$$|\rho_+\rangle\rangle = |I_+\rangle\rangle + \sum \chi_m |\hat{O}_{m,+}\rangle\rangle. \quad (\text{D4})$$

Here the coefficients χ_m and the N -body Pauli operators \hat{O}_m should be carefully chosen so that the corresponding ρ in the original Hilbert space represents a valid density matrix of the system.

We note that the operators \hat{O} can be classified into different groups according to the factors (δ_o, γ_o) defined in Eqs. (C21) and (C22). Therefore, due to the two-valued properties of δ_o and γ_o , all the Pauli operators \hat{O} can be divided into four

categories (\hat{A} , \hat{B} , \hat{C} , \hat{D}) and are listed as follows:

(1) Class A: $(\delta_o, \gamma_o) = (1, 1)$

$$\begin{aligned} |\hat{A} + \zeta \hat{A} \mathcal{M}\rangle\rangle &= |\hat{A}(1 + \zeta \mathcal{M})\rangle\rangle \\ &= |\hat{A}_+\rangle\rangle[(1 + \zeta)|1\rangle\rangle - (1 - \zeta)|0\rangle\rangle]; \end{aligned}$$

(2) Class B: $(\delta_o, \gamma_o) = (-1, 1)$

$$\begin{aligned} |-\zeta \hat{B} + \hat{B} \mathcal{M}\rangle\rangle &= |\hat{B} \mathcal{M}(1 - \zeta \mathcal{M})\rangle\rangle \\ &= |\hat{B}_+\rangle\rangle[-(1 + \zeta)|1\rangle\rangle + (1 - \zeta)|0\rangle\rangle]; \end{aligned}$$

(3) Class C: $(\delta_o, \gamma_o) = (1, -1)$

$$\begin{aligned} |\zeta \hat{C} + \hat{C} \mathcal{M}\rangle\rangle &= |\hat{C} \mathcal{M}(1 + \zeta \mathcal{M})\rangle\rangle \\ &= |\hat{C}_+\rangle\rangle[(1 + \zeta)|1\rangle\rangle - (1 - \zeta)|0\rangle\rangle]; \end{aligned}$$

(4) Class D: $(\delta_o, \gamma_o) = (-1, -1)$

$$\begin{aligned} |\hat{D} - \zeta \hat{D} \mathcal{M}\rangle\rangle &= |\hat{D}(1 - \zeta \mathcal{M})\rangle\rangle \\ &= |\hat{D}_+\rangle\rangle[(1 - \zeta)|0\rangle\rangle - (1 + \zeta)|1\rangle\rangle]. \end{aligned}$$

We also note that to ensure the Hermiticity of ρ , these operators $\{\hat{A}, \hat{B}, \hat{C}, \hat{D}\}$ also should be chosen to commute with \mathcal{M} . Therefore, the most general form of $|\rho_+\rangle\rangle$ reads

$$\begin{aligned} |\rho_+\rangle\rangle &= |I_+\rangle\rangle + \sum_i a_i |\hat{A}_{i,+}\rangle\rangle + \sum_j b_j |\hat{B}_{j,+}\rangle\rangle \\ &\quad + \sum_k c_k |\hat{C}_{k,+}\rangle\rangle + \sum_l d_l |\hat{D}_{l,+}\rangle\rangle, \end{aligned} \quad (\text{D5})$$

with real coefficients a_i , b_j , c_k , and d_l . The corresponding density matrix can be obtained accordingly,

$$\begin{aligned} \rho &= \frac{1}{2^N} \left[\left(I + \sum_i a_i \hat{A}_i + \sum_k c_k \hat{C}_k \mathcal{M} \right) (I + \zeta \mathcal{M}) \right. \\ &\quad \left. - \left(\sum_j b_j \hat{B}_j \mathcal{M} + \sum_l d_l \hat{D}_l \right) (I - \zeta \mathcal{M}) \right], \end{aligned} \quad (\text{D6})$$

where both the coefficients (a_i , b_j , c_k , d_l) and the operators (\hat{A}_i , \hat{B}_j , \hat{C}_k , \hat{D}_l) are carefully chosen so that ρ is a positive operator. In the special case with $b_j = d_l = 0$ for all j and l , the positivity of ρ is reduced to find (a_i, c_k) and (\hat{A}_i, \hat{C}_k) such that $(I + \sum_i a_i \hat{A}_i + \sum_k c_k \hat{C}_k \mathcal{M})$ is positive definite. For general case, to ensure the positivity of ρ , a sufficient condition can be chosen such that both $(I + \sum_i a_i \hat{A}_i + \sum_k c_k \hat{C}_k \mathcal{M})$ and $-(\sum_j b_j \hat{B}_j \mathcal{M} + \sum_l d_l \hat{D}_l)$ are positive operators.

We note that any Hermitian observable operator \hat{X} which maps to a product form in LFS can also be constructed following the above discussions. For instance, all operators defined in Eq. (D6) are product in LFS. If we choose the two operators \hat{X}_1 and \hat{X}_2 as $(\hat{X}_1, \hat{X}_2) = (\hat{O}, \hat{O} \mathcal{M})$, then the ratio $\langle \hat{X}_1 \rangle / \langle \hat{X}_2 \rangle$ can be simplified as

$$\frac{\langle X_1 \rangle}{\langle X_2 \rangle} = \frac{\langle \langle X_1 | \rho \rangle \rangle}{\langle \langle X_2 | \rho \rangle \rangle} = \frac{\delta_o + \gamma_o + \delta_o \zeta (\delta_o - \gamma_o)}{\delta_o - \gamma_o + \delta_o \zeta (\delta_o + \gamma_o)} = \delta_o \zeta^{-\delta_o}, \quad (\text{D7})$$

where in the last step, we have used the two-valued properties of δ_o and γ_o . Therefore, $\langle \hat{X}_1 \rangle / \langle \hat{X}_2 \rangle$ is time-independent during

the evolution for an initial product state. This can be used to clarify the existence of LMEMs in this dissipative system.

The edge modes are topologically protected by the internal symmetry of the system. The influences of perturbations on the system can be characterized by introducing additional interaction H' to the Hamiltonian H , or new dissipator L' into the Lindblad equation. The edge modes are decoupled from the bulk modes as long as the corresponding Lindbladians $X_{H'}$ and $X_{L'}$ in LFS are commuted with κ_1 and κ_{4N} , namely, $[X_{H'}, \kappa_1] = [X_{H'}, \kappa_{4N}] = [X_{L'}, \kappa_1] = [X_{L'}, \kappa_{4N}] = 0$. Since

$$\kappa_1 |\rho\rangle\rangle \rightarrow -\sigma_1^x \mathcal{M} \rho \mathcal{M} \sigma_1^x, \quad (\text{D8})$$

$$\kappa_{4N} |\rho\rangle\rangle \rightarrow i \sigma_N^x \rho \mathcal{M} \sigma_N^x, \quad (\text{D9})$$

$$X_{H'} |\rho\rangle\rangle \rightarrow [H', \rho], \quad (\text{D10})$$

$$X_{L'} |\rho\rangle\rangle \rightarrow 2L'^\dagger \rho L' - L' L'^\dagger \rho - \rho L' L'^\dagger, \quad (\text{D11})$$

using the spin language, we can rewrite $[X_{H'}, \kappa_1] |\rho\rangle\rangle = 0$ as

$$[\mathcal{M} \sigma_1^x H' \sigma_1^x \mathcal{M} - H', \rho] = 0, \quad (\text{D12})$$

which is valid for any given density matrix ρ . This leads to the following constraints for H' as

$$[H', \sigma_N^x] = [H', \sigma_1^x] = [H', \mathcal{M}] = 0. \quad (\text{D13})$$

Similar discussions also hold for additional dissipator L' by noticing $[X_{L'}, \kappa_1] |\rho\rangle\rangle = 0$, and we have

$$\begin{aligned} &2(\mathcal{M} \sigma_1^x L'^\dagger \sigma_1^x \mathcal{M} \rho \mathcal{M} \sigma_1^x L' \sigma_1^x \mathcal{M} - L'^\dagger \rho L') \\ &\quad - (\mathcal{M} \sigma_1^x L' L'^\dagger \sigma_1^x \mathcal{M} - L' L'^\dagger) \rho \\ &\quad - \rho (\mathcal{M} \sigma_1^x L' L'^\dagger \sigma_1^x \mathcal{M} - L' L'^\dagger) = 0. \end{aligned} \quad (\text{D14})$$

To ensure that the above identity holds for any density matrix ρ , we have

$$[L', \sigma_N^x] = [L', \sigma_1^x] = [L', \mathcal{M}] = 0. \quad (\text{D15})$$

In the main text, the existence of LMEMs is verified for different initial states and observables. Both of them can be re-expressed as bulk-edge product vectors in LFS. Specifically, for $N = 8$ and $\rho_0 = [I + \sum_{j=2}^{N-1} 0.2(\sigma_j^x \sigma_{j+1}^x + \sigma_j^z)] (I + 0.5 \prod_{j=1}^N \sigma_j^z) / 2^N$, all the corresponding operators $M_j = \sigma_j^x \sigma_{j+1}^x + \sigma_j^z$ ($2 \leq j \leq N - 1$) satisfy $(\delta_M, \gamma_M) = (1, 1)$ and belongs to A-class discussed above. The relevant vector of ρ_0 is product and reads

$$|\rho_0\rangle\rangle = (|I_+\rangle\rangle + 0.2 \sum_{j=2}^{N-1} |M_{j,+}\rangle\rangle)(1.5|1\rangle\rangle - 0.5|0\rangle\rangle) / 2^N, \quad (\text{D16})$$

with $\zeta = 0.5$, and $M_j = \sigma_j^x \sigma_{j+1}^x + \sigma_j^z$. Similarly, using the maps

$$\sigma_j^z \implies |\sigma_{j,+}^z\rangle\rangle(|1\rangle\rangle - |0\rangle\rangle), \quad (j \neq 1, N), \quad (\text{D17})$$

$$\sigma_j^x \sigma_{j+1}^x \implies |(\sigma_j^x \sigma_{j+1}^x)_+\rangle\rangle(|1\rangle\rangle - |0\rangle\rangle), \quad (\text{D18})$$

we can find that the relevant vectors in LFS for observables $X_1 = \sum_{j=2}^{N-1} (\sigma_j^x \sigma_{j+1}^x + \sigma_j^z) \mathcal{M}$ and $X_2 = X_1 \mathcal{M}$ can be written

as

$$|X_1\rangle\rangle = |M_+\rangle\rangle(|1\rangle\rangle + |0\rangle\rangle), \quad (\text{D19})$$

$$|X_2\rangle\rangle = |M_+\rangle\rangle(|1\rangle\rangle - |0\rangle\rangle), \quad (\text{D20})$$

where

$$|M_+\rangle\rangle = \left| \sum_{j=2}^{N-1} (\sigma_j^x \sigma_{j+1}^x + \sigma_j^z)_+ \right\rangle\rangle. \quad (\text{D21})$$

APPENDIX E: CORRELATION $\langle\langle ik_1 \kappa_{4N} \rangle\rangle$ IN LFS AND THE PURITY OF ρ

In this Appendix, we show that the correlation $\langle\langle ik_1 \kappa_{4N} \rangle\rangle$ defined in LFS is closely linked with the purity $\text{Tr}(\rho^2)$ of the density matrix ρ . We also show how the correlation can be detected using only local observables in spin basis.

Since any density matrix ρ can be expanded using pairs of Pauli operators $(\hat{O}_j, \hat{O}_j \mathcal{M})$, the corresponding vector in LFS can always be written as

$$|\rho\rangle\rangle = \sum_j r_j |\rho_j\rangle\rangle = \sum_j r_j |\hat{O}_{j,+}\rangle\rangle (a_j |1\rangle\rangle + b_j |0\rangle\rangle). \quad (\text{E1})$$

Therefore, the occupation number $\langle\langle \rho(t) | d_e^\dagger d_e | \rho(t) \rangle\rangle$ of the edge mode for the given vector $|\rho(t)\rangle\rangle$ in LFS reads

$$\begin{aligned} \langle\langle \rho(t) | d_e^\dagger d_e | \rho(t) \rangle\rangle &= \sum_{ij} r_i^* r_j \langle\langle \rho_i | d_e^\dagger d_e | \rho_j \rangle\rangle \\ &= \sum_{ij} r_i^* r_j a_i^* a_j \langle\langle \hat{O}_{i,+} | \hat{O}_{j,+} \rangle\rangle. \end{aligned} \quad (\text{E2})$$

Using the relations $\langle\langle \hat{O}_{i,+} | \hat{O}_{j,+} \rangle\rangle = 2^{N-1} \delta_{ij}$ and $ik_1 \kappa_{4N} = 2c_e^\dagger c_e - 1$, we immediately obtain

$$\langle\langle \rho(t) | ik_1 \kappa_{4N} | \rho(t) \rangle\rangle = 2^{N-1} \sum_i r_i^2 (a_i^2 - b_i^2). \quad (\text{E3})$$

Meanwhile, the purity $\text{Tr}(\rho^2)$ of the density matrix ρ can be re-expressed in LFS as

$$\langle\langle \rho(t) | \rho(t) \rangle\rangle = \sum_{ij} r_i^* r_j \langle\langle \rho_i | \rho_j \rangle\rangle = 2^{N-1} \sum_i r_i^2 (a_i^2 + b_i^2). \quad (\text{E4})$$

This means that for bulk-edge product state in LFS with $(a_j, b_j) = (a, b)$ for all j , the correlation $\langle\langle ik_1 \kappa_{4N} \rangle\rangle = \langle\langle \rho(t) | ik_1 \kappa_{4N} | \rho(t) \rangle\rangle$ is directly linked with $\text{Tr}(\rho^2)$, and satisfies

$$\langle\langle ik_1 \kappa_{4N} \rangle\rangle = \frac{a^2 - b^2}{a^2 + b^2} \text{Tr}(\rho^2). \quad (\text{E5})$$

Specifically, for the initial state discussed in the main text,

$$\begin{aligned} \rho_0 &= \left[I + 0.3 \prod_{j=1}^N \sigma_j^z (\sigma_1^z + \sigma_1^y \sigma_2^x + \sigma_1^y \sigma_3^x + \sigma_2^z \sigma_2^x \sigma_3^x) \right] \\ &\quad * \left(I + \zeta \prod_{j=1}^N \sigma_j^z \right) / 2^N, \end{aligned} \quad (\text{E6})$$

the corresponding product vector in LFS can be written as

$$|\rho_0\rangle\rangle = |\rho_{0,+}\rangle\rangle \otimes [(1 + \zeta)|1\rangle\rangle - (1 - \zeta)|0\rangle\rangle] / 2^N \quad (\text{E7})$$

and

$$\begin{aligned} |\rho_{0,+}\rangle\rangle &= |L_+\rangle\rangle + 0.3 (|(\sigma_1^z)_+\rangle\rangle + |(\sigma_1^y \sigma_2^x)_+\rangle\rangle \\ &\quad + |(\sigma_1^y \sigma_3^x)_+\rangle\rangle + |(\sigma_2^z \sigma_2^x \sigma_3^x)_+\rangle\rangle). \end{aligned} \quad (\text{E8})$$

This state has nonzero components in subspaces defined by $\{p_j = 1(\forall j)\}$ and $\{p_{j \neq 1} = 1(\forall j), p_1 = -1\}$.

For larger γ , the eigenvectors of \mathcal{L} for eigenvalue λ with the minimum $|\text{Im}(\lambda)| > 0$ are degenerate in the subspace $\{p_{j \neq 1} = 1(\forall j), p_1 = -1\}$ and read

$$\rho_1^0 = (\alpha \sigma_1^z + \sigma_1^y \sigma_2^x) \prod_{j=1}^N \sigma_j^z, \quad (\text{E9})$$

$$\rho_1^1 = \alpha \sigma_1^y \sigma_2^x + \sigma_1^z, \quad (\text{E10})$$

with $\alpha = (i\gamma \pm \sqrt{\gamma^2 - J^2})/J$. The above excited states and the stationary state can then be viewed as the combinations of following operators:

$$M = \left\{ I, \prod_i \sigma_i^z, \sigma_1^y \sigma_2^x, \sigma_1^z \right\} \cup \left\{ I, \prod_i \sigma_i^z, \sigma_1^y \sigma_2^x, \sigma_1^z \right\} \prod_i \sigma_i^z.$$

The purity $\text{Tr}(\rho^2)$ can be approximated as

$$\langle\langle \rho | \rho \rangle\rangle = \text{Tr}(\rho^2) \simeq \frac{1}{2^N} \sum_{O_i \in M} \langle O_i \rangle^2. \quad (\text{E11})$$

For the given initial state $|\rho_0\rangle\rangle$, since the following relations hold,

$$\left\langle \sigma_1^y \sigma_2^x \prod_i \sigma_i^z \right\rangle = \zeta \langle \sigma_1^y \sigma_2^x \rangle, \quad (\text{E12})$$

$$\left\langle \sigma_1^z \prod_i \sigma_i^z \right\rangle = \zeta \langle \sigma_1^z \rangle, \quad (\text{E13})$$

$$\left\langle \prod_i \sigma_i^z \right\rangle = \zeta, \quad (\text{E14})$$

we finally have

$$\langle\langle \rho | ik_1 \kappa_{2N} | \rho \rangle\rangle \simeq \frac{1}{2^{N-1}} \zeta (1 + \langle \sigma_1^z \rangle^2 + \langle \sigma_1^y \sigma_2^x \rangle^2). \quad (\text{E15})$$

- [1] T. Ozawa and H. M. Price, Topological quantum matter in synthetic dimensions, *Nat. Rev. Phys.* **1**, 349 (2019).
 [2] X.-W. Luo, X. Zhou, C.-F. Li, J.-S. Xu, G.-C. Guo, and Z.-W. Zhou, Quantum simulation of 2D topological physics in a 1D array of optical cavities, *Nat. Commun.* **6**, 7704 (2015).

- [3] C.-E. Bardyn and A. İmamoğlu, Majorana-like modes of light in a one-dimensional array of nonlinear cavities, *Phys. Rev. Lett.* **109**, 253606 (2012).
 [4] A. Stern and N. H. Lindner, Topological quantum computation—From basic concepts to first experiments, *Science* **339**, 1179 (2013).

- [5] D.-W. Zhang, Y.-Q. Zhu, Y. Zhao, H. Yan, and S.-L. Zhu, Topological quantum matter with cold atoms, *Adv. Phys.* **67**, 253 (2018).
- [6] N. Goldman, J. C. Budich, and P. Zoller, Topological quantum matter with ultracold gases in optical lattices, *Nat. Phys.* **12**, 639 (2016).
- [7] T. Karzig, C. Knapp, R. M. Lutchyn, P. Bonderson, M. B. Hastings, C. Nayak, J. Alicea, K. Flensberg, S. Plugge, Y. Oreg *et al.*, Scalable designs for quasiparticle-poisoning-protected topological quantum computation with Majorana zero modes, *Phys. Rev. B* **95**, 235305 (2017).
- [8] T. Hyart, B. van Heck, I. C. Fulga, M. Burrello, A. R. Akhmerov, and C. W. J. Beenakker, Flux-controlled quantum computation with Majorana fermions, *Phys. Rev. B* **88**, 035121 (2013).
- [9] J. Alicea, Y. Oreg, G. Refael, F. Von Oppen, and M. P. Fisher, Non-Abelian statistics and topological quantum information processing in 1D wire networks, *Nat. Phys.* **7**, 412 (2011).
- [10] J. Fraxanet, D. González-Cuadra, T. Pfau, M. Lewenstein, T. Langen, and L. Barbiero, Topological quantum critical points in the extended Bose-Hubbard model, *Phys. Rev. Lett.* **128**, 043402 (2022).
- [11] B. Yan and S.-C. Zhang, Topological materials, *Rep. Prog. Phys.* **75**, 096501 (2012).
- [12] D. Culcer, A. C. Keser, Y. Li, and G. Tkachov, Transport in two-dimensional topological materials: Recent developments in experiment and theory, *2D Mater.* **7**, 022007 (2020).
- [13] B. A. Bernevig, C. Felser, and H. Beidenkopf, Progress and prospects in magnetic topological materials, *Nature (London)* **603**, 41 (2022).
- [14] H. Pichler, A. J. Daley, and P. Zoller, Nonequilibrium dynamics of bosonic atoms in optical lattices: Decoherence of many-body states due to spontaneous emission, *Phys. Rev. A* **82**, 063605 (2010).
- [15] L.-L. Yan, J.-W. Zhang, M.-R. Yun, J.-C. Li, G.-Y. Ding, J.-F. Wei, J.-T. Bu, B. Wang, L. Chen, S.-L. Su *et al.*, Experimental verification of dissipation-time uncertainty relation, *Phys. Rev. Lett.* **128**, 050603 (2022).
- [16] D. Poletti, P. Barmettler, A. Georges, and C. Kollath, Emergence of glasslike dynamics for dissipative and strongly interacting bosons, *Phys. Rev. Lett.* **111**, 195301 (2013).
- [17] Z. Cai and T. Barthel, Algebraic versus exponential decoherence in dissipative many-particle systems, *Phys. Rev. Lett.* **111**, 150403 (2013).
- [18] N. Syassen, D. M. Bauer, M. Lettner, T. Volz, D. Dietze, J. J. Garcia-Ripoll, J. I. Cirac, G. Rempe, and S. Dürr, Strong dissipation inhibits losses and induces correlations in cold molecular gases, *Science* **320**, 1329 (2008).
- [19] K. Sponselee, L. Freystatzky, B. Abeln, M. Diem, B. Hundt, A. Kochanek, T. Ponath, B. Santra, L. Mathey, K. Sengstock *et al.*, Dynamics of ultracold quantum gases in the dissipative Fermi-Hubbard model, *Quantum Sci. Technol.* **4**, 014002 (2018).
- [20] M. J. Schmidt, D. Rainis, and D. Loss, Decoherence of Majorana qubits by noisy gates, *Phys. Rev. B* **86**, 085414 (2012).
- [21] T. Tomita, S. Nakajima, I. Danshita, Y. Takasu, and Y. Takahashi, Observation of the Mott insulator to superfluid crossover of a driven-dissipative Bose-Hubbard system, *Sci. Adv.* **3**, e1701513 (2017).
- [22] B. Scioffa, D. Poletti, and C. Kollath, Two-time correlations probing the dynamics of dissipative many-body quantum systems: Aging and fast relaxation, *Phys. Rev. Lett.* **114**, 170401 (2015).
- [23] L. Henriot, J. S. Douglas, D. E. Chang, and A. Albrecht, Critical open-system dynamics in a one-dimensional optical-lattice clock, *Phys. Rev. A* **99**, 023802 (2019).
- [24] K. Seetharam, A. Lerose, R. Fazio, and J. Marino, Correlation engineering via nonlocal dissipation, *Phys. Rev. Res.* **4**, 013089 (2022).
- [25] R. Bouganne, M. B. Aguilera, A. Ghermaoui, J. Beugnon, and F. Gerbier, Anomalous decay of coherence in a dissipative many-body system, *Nat. Phys.* **16**, 21 (2020).
- [26] S. Diehl, E. Rico, M. A. Baranov, and P. Zoller, Topology by dissipation in atomic quantum wires, *Nat. Phys.* **7**, 971 (2011).
- [27] C.-E. Bardyn, M. A. Baranov, C. V. Kraus, E. Rico, A. İmamoğlu, P. Zoller, and S. Diehl, Topology by dissipation, *New J. Phys.* **15**, 085001 (2013).
- [28] F. Verstraete, M. M. Wolf, and J. I. Cirac, Quantum computation and quantum-state engineering driven by dissipation, *Nat. Phys.* **5**, 633 (2009).
- [29] P. San-Jose, J. Cayao, E. Prada, and R. Aguado, Majorana bound states from exceptional points in non-topological superconductors, *Sci. Rep.* **6**, 21427 (2016).
- [30] H. Shen, B. Zhen, and L. Fu, Topological band theory for non-Hermitian Hamiltonians, *Phys. Rev. Lett.* **120**, 146402 (2018).
- [31] Z. Gong, Y. Ashida, K. Kawabata, K. Takasan, S. Higashikawa, and M. Ueda, Topological phases of non-Hermitian systems, *Phys. Rev. X* **8**, 031079 (2018).
- [32] F. Song, S. Yao, and Z. Wang, Non-Hermitian topological invariants in real space, *Phys. Rev. Lett.* **123**, 246801 (2019).
- [33] N. Okuma, K. Kawabata, K. Shiozaki, and M. Sato, Topological origin of non-hermitian skin effects, *Phys. Rev. Lett.* **124**, 086801 (2020).
- [34] A. Ghatak and T. Das, New topological invariants in non-Hermitian systems, *J. Phys.: Condens. Matter* **31**, 263001 (2019).
- [35] D. S. Borgnia, A. J. Kruchkov, and R.-J. Slager, Non-Hermitian boundary modes and topology, *Phys. Rev. Lett.* **124**, 056802 (2020).
- [36] A. Maiellaro, F. Romeo, and F. Illuminati, Edge states, Majorana fermions, and topological order in superconducting wires with generalized boundary conditions, *Phys. Rev. B* **106**, 155407 (2022).
- [37] L. M. Vasiloiu, F. Carollo, and J. P. Garrahan, Enhancing correlation times for edge spins through dissipation, *Phys. Rev. B* **98**, 094308 (2018).
- [38] L. M. Vasiloiu, A. Tiwari, and J. H. Bardarson, Dephasing-enhanced Majorana zero modes in two-dimensional and three-dimensional higher-order topological superconductors, *Phys. Rev. B* **106**, L060307 (2022).
- [39] T. Van Vu and K. Saito, Finite-time quantum landauer principle and quantum coherence, *Phys. Rev. Lett.* **128**, 010602 (2022).
- [40] V. V. Albert and L. Jiang, Symmetries and conserved quantities in Lindblad master equations, *Phys. Rev. A* **89**, 022118 (2014).
- [41] R. Chetrite and K. Mallick, Quantum fluctuation relations for the Lindblad master equation, *J. Stat. Phys.* **148**, 480 (2012).
- [42] T. Prosen, Third quantization: A general method to solve master equations for quadratic open Fermi systems, *New J. Phys.* **10**, 043026 (2008).

- [43] T. Prosen, Spectral theorem for the Lindblad equation for quadratic open fermionic systems, *J. Stat. Mech.* (2010) P07020.
- [44] T. Prosen and B. Žunkovič, Exact solution of Markovian master equations for quadratic Fermi systems: Thermal baths, open XY spin chains and non-equilibrium phase transition, *New J. Phys.* **12**, 025016 (2010).
- [45] A. J. Daley, Quantum trajectories and open many-body quantum systems, *Adv. Phys.* **63**, 77 (2014).
- [46] M. de Leeuw, C. Paletta, and B. Pozsgay, Constructing integrable Lindblad superoperators, *Phys. Rev. Lett.* **126**, 240403 (2021).
- [47] A. Y. Kitaev, Unpaired Majorana fermions in quantum wires, *Phys. Usp.* **44**, 131 (2001).
- [48] J. Reslen, Uncoupled Majorana fermions in open quantum systems: On the efficient simulation of non-equilibrium stationary states of quadratic Fermi models, *J. Phys.: Condens. Matter* **32**, 405601 (2020).
- [49] A. Carmele, M. Heyl, C. Kraus, and M. Dalmonte, Stretched exponential decay of Majorana edge modes in many-body localized Kitaev chains under dissipation, *Phys. Rev. B* **92**, 195107 (2015).
- [50] M. Goldstein, Dissipation-induced topological insulators: A no-go theorem and a recipe, *SciPost Phys.* **7**, 067 (2019).
- [51] Y. Huang, A. M. Lobos, and Z. Cai, Dissipative Majorana quantum wires, *iScience* **21**, 241 (2019).
- [52] N. Shibata and H. Katsura, Dissipative quantum Ising chain as a non-Hermitian Ashkin-Teller model, *Phys. Rev. B* **99**, 224432 (2019).
- [53] N. Shibata and H. Katsura, Dissipative spin chain as a non-Hermitian Kitaev ladder, *Phys. Rev. B* **99**, 174303 (2019).
- [54] R. Islam, R. Ma, P. M. Preiss, M. E. Tai, A. Lukin, M. Rispoli, and M. Greiner, Measuring entanglement entropy in a quantum many-body system, *Nature (London)* **528**, 77 (2015).
- [55] D. A. Abanin and E. Demler, Measuring entanglement entropy of a generic many-body system with a quantum switch, *Phys. Rev. Lett.* **109**, 020504 (2012).
- [56] J. Cardy, Measuring entanglement using quantum quenches, *Phys. Rev. Lett.* **106**, 150404 (2011).
- [57] A. Elben, B. Vermersch, M. Dalmonte, J. I. Cirac, and P. Zoller, Rényi entropies from random quenches in atomic Hubbard and spin models, *Phys. Rev. Lett.* **120**, 050406 (2018).
- [58] M. B. Hastings, I. González, A. B. Kallin, and R. G. Melko, Measuring Rényi entanglement entropy in quantum Monte Carlo simulations, *Phys. Rev. Lett.* **104**, 157201 (2010).
- [59] T. Rakovszky, F. Pollmann, and C. W. von Keyserlingk, Sub-ballistic growth of Rényi entropies due to diffusion, *Phys. Rev. Lett.* **122**, 250602 (2019).